

Maturation of mouse NK cells is a 4-stage developmental program

Laura Chiossone,¹⁻³ Julie Chaix,¹⁻³ Nicolas Fuseri,⁴ Claude Roth,⁵ Eric Vivier,^{1-3,6} and Thierry Walzer¹⁻³

¹Centre d'Immunologie de Marseille-Luminy, Université de la Méditerranée, Marseille; ²Inserm, U631, Marseille; ³Centre National de la Recherche Scientifique (CNRS), UMR6102, Marseille; ⁴Innate-Pharma, Marseille; ⁵Département d'Immunologie, Institut Pasteur, Paris; and ⁶Assistance Publique-Hôpitaux (AP-HP) de Marseille, Hôpital de la Conception, Marseille, France

Surface density of CD27 and CD11b subdivides mouse natural killer (NK) cells into 4 subsets: CD11b^{low}CD27^{low}, CD11b^{low}CD27^{high}, CD11b^{high}CD27^{high}, and CD11b^{high}CD27^{low}. To determine the developmental relationship between these 4 subsets, we used several complementary approaches. First, we took advantage of NDE transgenic mice that express enhanced green fluorescent protein (EGFP) and diphtheria toxin receptor specifically in NK cells. Diphtheria toxin in-

jection leads to a transient depletion of NK cells, allowing the monitoring of the phenotype of developing EGFP⁺ NK cells after diphtheria toxin injection. Second, we evaluated the overall proximity between NK-cell subsets based on their global gene profile. Third, we compared the proliferative capacity of NK-cell subsets at steady state or during replenishment of the NK-cell pool. Fourth, we performed adoptive transfers of EGFP⁺ NK cell subsets from NDE mice into unir-

radiated mice and followed the fate of transferred cells. The results of these various experiments collectively support a 4-stage model of NK-cell maturation CD11b^{low}CD27^{low} → CD11b^{low}CD27^{high} → CD11b^{high}CD27^{high} → CD11b^{high}CD27^{low}. This developmental program appears to be associated with a progressive acquisition of NK-cell effector functions. (Blood. 2009;113:5488-5496)

Introduction

Natural killer (NK) cells are lymphocytes of the innate immunity with effector functions, such as perforin-dependent cytotoxicity and interferon- γ secretion. Several lines of evidence implicate them in the early control of virus infection, in tumor immunosurveillance, and in the regulation of immune responses.^{1,2} Mature NK cells express a wide variety of cell-surface receptors that enable them to recognize targets expressing low surface amounts of major histocompatibility complex class I molecules or high surface amounts of molecules induced by stress or microbial molecules.^{3,4} The NK-cell receptors specific for the major histocompatibility complex class I molecules include the human killer-cell Ig-like (KIR) and mouse Ly49 receptors, and CD94/NKG2 complexes in both species.⁵

NK cells are heterogeneous as to their phenotype, function, and anatomic distribution. In human, 2 subsets of NK cells differing by their level of CD56 expression have been identified and well characterized.⁶ CD56^{bright} NK cells are found mostly in lymphoid organs.⁷ They express few surface KIR molecules, are poorly cytolytic, but proliferate vigorously after interaction with activated dendritic cells. By contrast, CD56^{dim} NK cells are predominant in peripheral blood, express high levels of KIR molecules, and display potent cytotoxic function. It has long been proposed that CD56^{bright} NK cells were precursors of CD56^{dim} NK cells.⁸ In mice, 2 populations of NK cells with low and high expression of CD11b have been identified. In fetal and neonatal mice, CD11b^{low} NK cells composed most of the NK-cell population.⁹ In the adult, CD11b^{low} NK cells were found mostly in the bone marrow, lymph nodes, and liver and had a high rate of homeostatic proliferation. CD11b^{high} NK cells were present rather at peripheral sites, such as spleen, peripheral blood mononuclear cells (PBMCs), and lung. The latter

expressed high levels of Ly49 receptors and displayed potent effector functions compared with the CD11b^{low} NK cells.¹⁰ The CD11b^{high} NK-cell subset could be further dissected in 2 populations based on CD27 expression: CD11b^{high}CD27^{high} and CD11b^{high}CD27^{low} cells. CD11b^{high}CD27^{high} NK cells were found to be the most potent effector cells and responded better to CXCR3 or CXCR4 ligands in vitro.¹¹ CD11b^{high}CD27^{low} NK cells expressed Ly49 receptors at the highest frequency and expressed unique receptors for chemoattractants, such as CX3CR1¹² or S1P₅.¹³

It has been proposed that CD11b^{low}CD27^{high}, CD11b^{high}CD27^{high}, and CD11b^{high}CD27^{low} (referred to hereafter as CD11b^{low}, DP [for double-positive], and CD27^{low} NK cells, respectively) were discrete stages of in vivo maturation following the pathway CD11b^{low} → DP → CD27^{low}.^{11,14} Besides correlative evidence, the most compelling support for this model lies in adoptive transfer of sorted CD11b^{low} NK cells into irradiated recipient mice, which suggested that CD11b^{high} NK cells were derived from CD11b^{low} NK cells.^{9,10,14,15} However, irradiation of recipient mice is a harsh conditioning regimen that can impact on transferred cells by inducing their "homeostatic" proliferation and differentiation.¹⁶ Thus, whether subsets defined by CD11b and CD27 expression represent distinct NK-cell development stages has not been formally demonstrated yet.

We sought to address the developmental relationship between NK-cell subsets using a combination of 4 complementary approaches assessing the kinetics of appearance of each subset during development, their gene expression profile at the pan-genomic level, their rate of proliferation, and their potential to give rise to the other subsets in vivo. Our results show that NK-cell maturation

Submitted October 31, 2008; accepted February 16, 2009. Prepublished online as *Blood* First Edition paper, February 20, 2009; DOI 10.1182/blood-2008-10-187179.

The online version of this article contains a data supplement.

The publication costs of this article were defrayed in part by page charge payment. Therefore, and solely to indicate this fact, this article is hereby marked "advertisement" in accordance with 18 USC section 1734.

© 2009 by The American Society of Hematology

is a 4-stage process that starts at a CD11b^{low}CD27^{low} stage and leads them through the following stages: CD11b^{low}CD27^{high} → CD11b^{high}CD27^{high} → CD11b^{high}CD27^{low}.

Methods

Mice and NK-cell depletion

The generation of NDE mice has been described previously.¹⁷ More information on the characterization of these mice may be found on the CIML website (http://www.ciml.univ-mrs.fr/Lab/Vivier/Protocoles/NKDTR-EGFP_mice.pdf). These mice were 6 generations backcrossed to C57BL/6 mice. NDE mice with at least 80% enhanced green fluorescent protein (EGFP)-positive NK cells were selected for all the depletion experiments in this study. NK-cell depletion was obtained by intravenous injection of 2 μg per mouse of diphtheria toxin (DT; Calbiochem, La Jolla, CA). We verified that DT is short lived (24 hours) and does not induce adverse effects in NDE mice (data not shown). C57BL/6 mice and RAG-2 KO mice on C57BL/6 background were obtained from Charles River Laboratories (Les Oncins, France). All mice were used between 6 and 12 weeks of age unless specified. All experiments have been performed in accordance with protocols approved by the local ethical committee at Université de la Méditerranée.

Flow cytometry and lymphocyte preparation

Lymphocyte suspensions were prepared from different organs as described previously.¹⁷ For cell-surface staining, anti-CD16/CD32 (2.4G.2) hybridoma supernatant was added. NKp46 expression was detected using the rat 29A1.4 monoclonal antibody (mAb)¹⁷ coupled with Alexa 647 fluorochrome (Invitrogen, Carlsbad, CA). Pacific Blue anti-mouse CD3 complex was purchased from BioLegend (San Diego, CA). Phycoerythrin (PE)-Cy5 anti-mouse CD127, biotin anti-mouse NKG2D, and PE anti-mouse granzyme B were from eBioscience (San Diego, CA). All other antibodies were from BD Biosciences PharMingen (San Diego, CA). Streptavidin-peridinin chlorophyll protein from BD Biosciences PharMingen was used as a secondary reagent for biotinylated antibodies. Before intracellular staining, samples were treated with BD Cytotfix/Cytoperm and Perm/Wash solutions (BD Biosciences, San Jose, CA). Samples were run on a fluorescence-activated cell sorter (FACS) Canto II or a FACS LSR II cytometers (BD Biosciences) and analyzed using FlowJo 8.7 software (TreeStar, Ashland, OR).

Cell sorting and transfer

Lymphocytes obtained from spleen and liver of NDE mice were incubated for 20 minutes at 4°C with a cocktail of mAb: rat anti-mouse CD4 (H129.19), CD5 (53-7.3), and CD8 (H59.101.2; all hybridoma supernatants), purified anti-mouse I-A/I-E, and purified rat anti-mouse TER-119 (both from BD Biosciences PharMingen). Cells were then washed and incubated with BioMag goat anti-rat IgG-coated magnetic beads (Polysciences, Warrington, PA) for 45 minutes at 4°C. Cells attached to beads were removed with a magnetic separator. A total of 80% pure NK cells were obtained using this procedure. Cells were then incubated with PE-conjugated anti-CD27 antibody and PE-Cy7-conjugated anti-CD11b antibody. NK cells were identified as EGFP⁺ and sorted into different subsets using a FACS Aria Cell Sorter (BD Biosciences). Purity of sorted cell populations was more than 98% as checked by flow cytometry. For cell transfer, 8 × 10³ to 2 × 10⁵ sorted cells were injected intravenously into unirradiated wild-type littermate recipients. The presence of transferred cells was analyzed at days 7 and 14 after transfer by cytofluorimetric analysis of NK cell-enriched splenocytes. The expression of CD27 and CD11b was analyzed on CD19⁻ CD3⁻ NK1.1⁺ EGFP⁺ cells.

Measurement of BrdU incorporation

Mice were given 2 intraperitoneal injections of 0.5 mg bromodeoxyuridine (BrdU; BD Biosciences PharMingen) within a 2-hour interval. Six hours

after the first BrdU injection, mice were killed and organs harvested. Cells derived from the bone marrow were stained with mAb as described in "Flow cytometry and lymphocyte preparation." After fixation and permeabilization, cells were treated with DNase and stained with fluorescein isothiocyanate anti-BrdU mAb, according to the manufacturer's instructions. BrdU incorporation for different cell populations was measured by flow cytometry.

Gene profiling and data mining

NK-cell subsets were sorted by flow cytometry from RAG2^{-/-} mice. We determined that the distribution of NK-cell subsets in RAG2^{-/-} mice was similar to that in C57BL/6 mice. RNA was extracted from each sorted NK-cell subset with the QIAGEN (Courtaboeuf, France) micro-RNAeasy kit. Quality and absence of genomic DNA contamination were assessed with a Bioanalyzer (Agilent Technologies, Palo Alto, CA). RNA from each sample was used to synthesize probes, using 2 successive rounds of cRNA amplification with appropriate quality control to ensure full-length synthesis according to standard Affymetrix protocols, and hybridized to mouse 430 2.0 chips (Affymetrix, Santa Clara, CA). Raw data were transformed with the Robust Multiarray Analysis (RMA) algorithm to normalize expression value. The software Cluster and Treeview were used to identify differentially expressed genes (1.5 cutoff) and classify cell subsets according to the proximity of their gene expression pattern as assessed by hierarchical clustering with complete linkage. Gene lists were analyzed using the DAVID tools accessible on the National Institute of Allergy and Infectious Diseases website. Individual significant annotations encompassing many common genes or similar biologic processes were regrouped using the "Functional annotation clustering" tool of the DAVID software.¹⁸ More information on this type of analysis is available on the DAVID website. Microarray data have been deposited at the National Center for Biotechnology Information GEO repository under accession number GSE13229 (released in March 2009).¹⁹

Statistical analyses

Statistical analyses were performed using GraphPad Prism (GraphPad Software, San Diego, CA).

Results

CD11b and CD27 surface expression define 4 subsets of NK cells

As a first step to investigate the developmental relationship between mouse NK-cell subsets defined by CD27 and CD11b surface expression, we took advantage of EGFP expression in NDE transgenic mice (Figure 1A). Indeed, these mice express EGFP and DT receptor under the control of the promoter region of the NK-cell marker NKp46/NCR1/CD335.¹⁷ We verified that nearly all EGFP⁺ cells were also NK1.1⁺CD122⁺ (Figure 1A). Surprisingly, we found that the CD11b and CD27 staining dissected 4 subsets, including the aforementioned CD11b^{low}, DP, and CD27^{low} subsets¹¹ and an additional CD11b^{low}CD27^{low} or double-negative (DN) subset (Figure 1A). DN NK cells were clearly visible in previously published flow cytometry plots of CD11b and CD27 expression¹¹ but had not been characterized in detail. We therefore investigated their distribution and surface phenotype. DN NK cells were present at very low frequency in all lymphoid and nonlymphoid organs analyzed of NDE or C57BL/6 mice (Figure 1B and data not shown). They were not NK-like T cells²⁰ as they were also present in RAG^{-/-} mice (data not shown). DN cells expressed NK1.1, NKG2D, NKp46, and granzyme B at the same level as the other subsets (Figure 1C and data not shown). However, they expressed

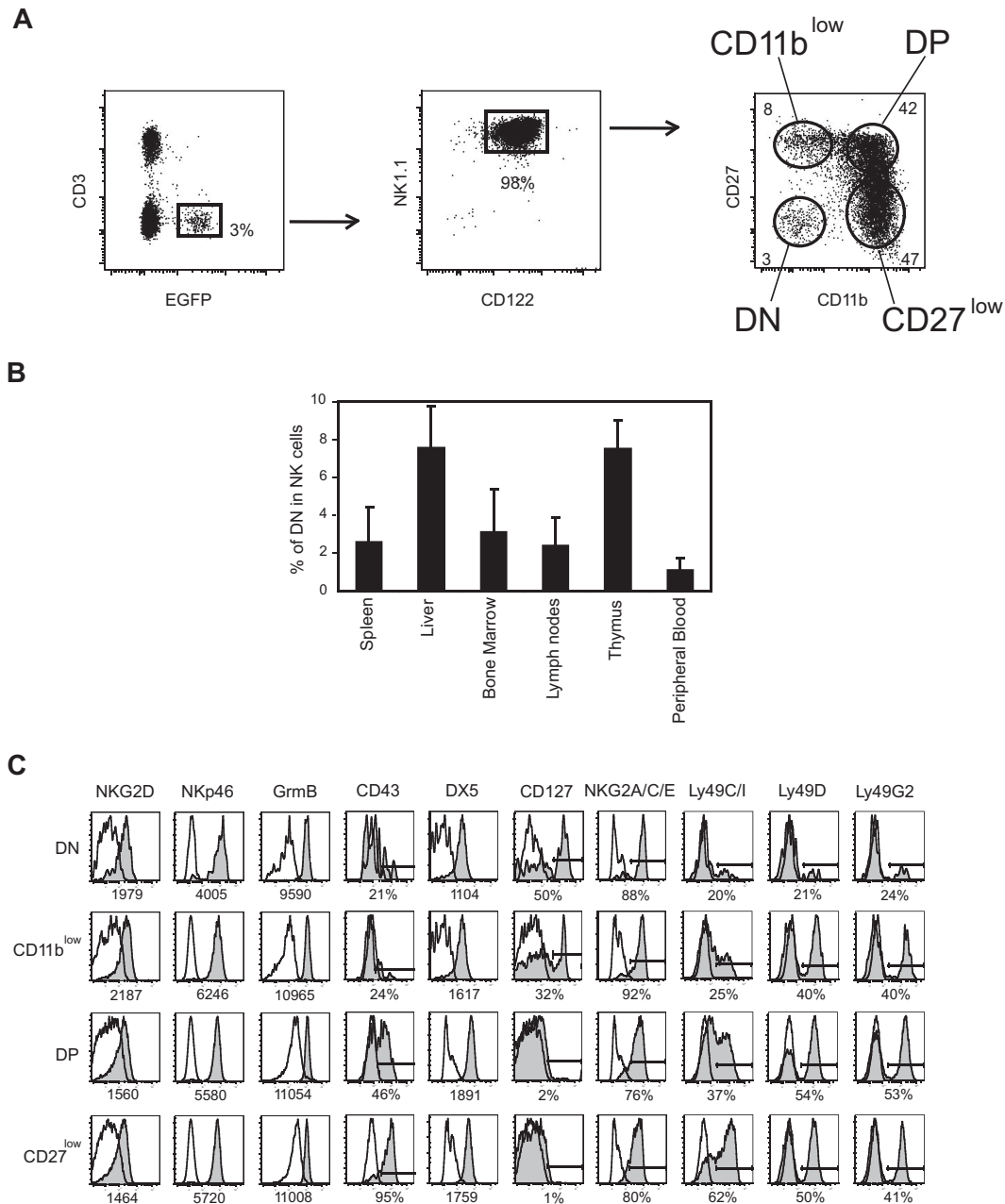


Figure 1. NK-cell differentiation includes DN NK cells. (A) Representative flow cytometry analysis of the expression of CD3, EGFP, CD122, NK1.1, CD27, and CD11b by splenic lymphocytes of NDE mice showing the gates used to identify NK cells and NK-cell subsets defined by CD27/CD11b expression. (B) Frequency of DN NK cells among total NK cells from different organs of NDE mice; n = 4 to 30 mice. (C) Expression of various cell-surface or intracellular molecules by gated splenic DN NK cells versus the other NK-cell subsets. Results are representative of 3 experiments.

low levels of Ly49 receptors, low levels of CD43 and DX5 (CD49b), but reciprocally high levels of interleukin-7 (IL-7) receptor (CD127), and NKG2A/C/E surface proteins compared with the other NK-cell subsets (Figure 1C). Thus, DN NK cells may represent immature NK cells present in various numbers in bone marrow and peripheral sites, such as spleen, liver, lymph nodes, thymus, and peripheral blood.

DN, CD11b^{low}, DP, and CD27^{low} NK cells develop sequentially in NDE mice after DT injection or during development of C57BL/6 mice

We previously described that DT injection leads to a transient depletion of EGFP⁺ NK cells in NDE mice.¹⁷ Complete depletion

of NK cells occurs in 3 days. EGFP⁺ NK cells start to reappear at day 4 after DT injection, and complete reconstitution takes 3 to 4 weeks (Figure S1A, available on the *Blood* website; see the Supplemental Materials link at the top of the online article; and data not shown). We took advantage of this unique model to investigate the kinetics of appearance of each NK-cell subset during reconstitution. For this, we monitored the expression of CD27 and CD11b by EGFP⁺ NK cells from different organs at various times after DT injection. Our results show that the CD11b and CD27 profiles of EGFP⁺ NK cells changed drastically over time, as illustrated for spleen NK cells in Figure 2A.

When looking at the frequency of each subset among NK cells at different times after DT injection (Figure 2B), several observations can

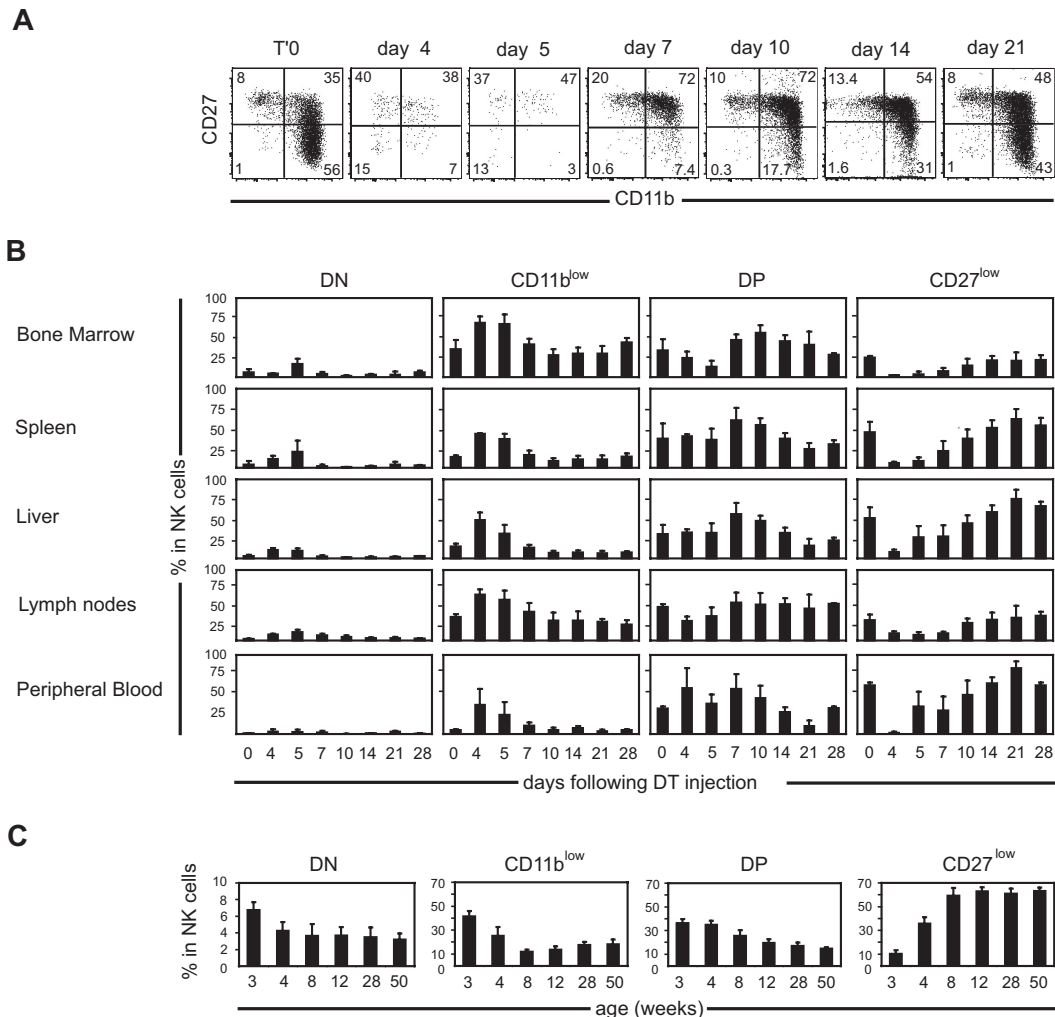


Figure 2. Kinetics of occurrence of NK-cell subsets after DT-induced depletion in NDE mice. (A) Representative flow cytometric analysis of CD27/CD11b expression by splenic NK cells over time after DT-induced depletion. (B) Frequency of each subset in NK cells of different organs, over time after DT-induced depletion, as calculated from flow cytometry data; $n = 3$ to 8 mice for each time point. (C) Frequency of each subset in splenic NK cells isolated from C57BL/6 mice of different ages; $n = 3$ or 4 for each time point.

be made. (1) At early time points (days 4 and 5), the DN and CD11b^{low} fractions were overrepresented compared with the later time points. (2) In a second phase (days 7–10), DP NK cells predominated in NK cells from all organs; and (3) in the later phase of the kinetics (days 14–28), CD27^{low} NK cells progressively represented the majority of the cells, especially in the spleen, liver, and PBMCs. When looking at cell numbers in the spleen and bone marrow (Figure S1B), a similar phenomenon was observed, namely, that DN/CD11b^{low} NK cells were overrepresented at day 5, whereas DP and later CD27^{low} NK cells successively accumulated. Next, we wanted to determine whether similar kinetics also occurred during the development of the NK-cell pool in the first weeks of life. To test this, we investigated the CD11b and CD27 phenotypes of splenic NK cells of wild-type mice of different ages. As shown in Figure 2C, the frequency of DN and CD11b^{low} subsets in NK cells was very high at early (3–4 weeks) time points. The frequency of DP NK cells was also high at early time points but decreased more slowly to reach homeostasis at 12 weeks of age. Finally, the frequency of CD27^{low} NK cells rose progressively and started to plateau at 8 to 12 weeks of age. Altogether, these results show that, after DT-induced depletion or during normal development in wild-type mice, DN and CD11b^{low} NK cells arise first, before DP and CD27^{low} NK cells, which accumulate gradually during consecutive phases.

Global transcriptomic analyses support a CD11b^{low} → DP → CD27^{low} pathway of differentiation

To confirm the relevance of CD11b/CD27 cell-surface expression in the identification of NK-cell subsets, we compared the gene expression profile of flow cytometry–sorted NK-cell subsets using pan-genomic microarrays. This analysis was restricted to CD11b^{low}, DP, and CD27^{low} NK cells because DN NK-cell numbers were too limiting for this type of experiment. We performed a hierarchical clustering with complete linkage of differentially expressed genes (Figure 3A). Differentially expressed genes were represented in only 5 clusters, of which 2 (clusters I and IV, Figure 3A) predominated (39% and 43% of differential probe sets, respectively; Figure 3A). Strikingly, clusters I and IV, which included 466 and 341 probe sets, respectively (Table S1), corresponded to genes that followed either the relationship CD11b^{low} > DP > CD27^{low} or the reverse relationship, CD27^{low} > DP > CD11b^{low}. These data thus provided a strong supportive evidence of both the relevance of CD11b/CD27 cell-surface phenotype as markers of NK-cell differentiation and the CD11b^{low} → DP → CD27^{low} model of differentiation.

This pan-genomic analysis also permitted mining for “unbiased” functional differences between NK-cell subsets, focusing on

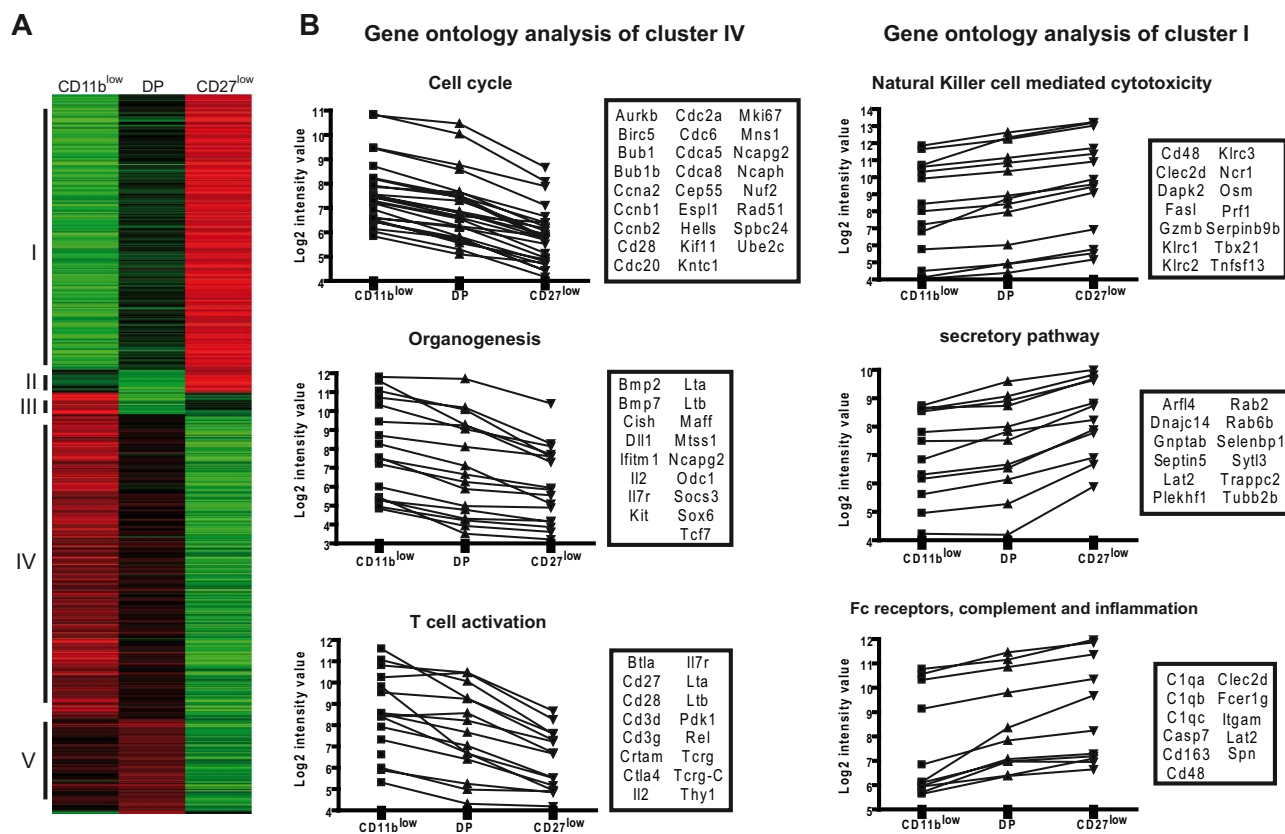


Figure 3. Gene profiling experiments reveal a dissociation between proliferation and effector functions in maturing NK cells. Gene expression profiles of sorted NK-cell subsets ($n = 2$ for each subset) were generated using pan-genomic microarrays. (A) Differentially expressed genes were identified and clustered according to their expression profile. The different clusters were numbered I to V. (B) A gene ontology analysis was performed on genes of the clusters I and IV. Highly significant terms are shown with the associated genes (boxes) and their expression profile in the 3 NK-cell subsets.

the 2 main clusters of differentially expressed genes (clusters I and IV). For each cluster ($CD11b^{low} > DP > CD27^{low}$ and $CD27^{low} > DP > CD11b^{low}$), we analyzed the gene ontology terms using DAVID data mining tools that include gene ontology analyses and PubMed searches¹⁸ (Table S2). “Cell cycle” was by far the most statistically significant term associated with the $CD11b^{low}$ NK-cell signature (cluster IV), as a large fraction of the corresponding genes were involved in cell cycle, such as cyclins and cyclin-dependent kinases, in chromosome condensation or in microtubule-based movement (Figure 3B). Moreover, when we focused on the transcription factors differentially expressed by $CD11b^{low}$ and $CD27^{low}$ subsets (Tables 1,2), we found in the $CD11b^{low}$ cluster, proto-oncogenes, such as *Myc* and *Rel*, as well as genes that have been associated with clonogenic potential in lymphocytes, such as *Myb*,²¹ or in pluripotency, such as *Klf4*.²² Less significantly, the analysis of the gene signature of $CD11b^{low}$ NK cells also revealed their expression of several transcripts associated with organogenesis or T-cell activation (Figure 3B). The “organogenesis” cluster contained genes, such as lymphotoxins α and β , which are also expressed at high levels by lymphoid tissue inducer cells or by gut $CD3^{-}NKp46^{+}$ cells.²³ The “T-cell activation” cluster contains genes shared with the T-cell lineage, such as IL-7 receptors and CD27 and somatic T-cell receptor- γ/δ transcripts, which have been previously shown to be expressed by NK cells.²⁰

Conversely to $CD11b^{low}$ NK cells, the most statistically significant terms associated with $CD27^{low}$ NK cells were relevant to effector functions (Table S2; Figure 3B). In particular, several of the most important genes in NK cell-mediated cytotoxicity, such as

granzyme B, perforin, and various NK-cell receptors, were up-regulated in $CD27^{low}$ NK cells (Figure 3B). A large fraction of genes involved in the secretory pathway, such as Rab proteins, were also up-regulated in this subset and may correspond to genes involved in the trafficking of cytotoxic granules. These results correlated with the high expression by $CD27^{low}$ NK cells of the T-bet (*Tbx21*) transcription factor (Tables 1,2), which has been shown to be required for the cytotoxic function.²⁴ A further look at the $CD27^{low}$ signature (Table S1) also revealed the presence of various molecules involved in trafficking (*CX3CR1*), cell-cell adhesion (*ITGAM*, *JAM4*, *MCAM*), cytokine response (*IL-12* receptor), or in the induction of inflammation (chemokines *CCL3*, *CCL4*), further highlighting the “effector” nature of the DP and $CD27^{low}$ NK-cell subsets. Thus, according to gene ontology analysis, $CD11b^{low}$ and $CD27^{low}$ NK cells largely differ by their specialization in proliferation and effector functions, respectively.

DN NK cells display the highest rate of homeostatic proliferation among NK-cell subsets

Next, we compared the capacity of NK-cell subsets to proliferate at steady state or during development of the NK-cell pool. For this, NDE mice first received DT or phosphate-buffered saline. Seven days later, mice were given BrdU twice at 3-hour intervals, and BrdU incorporation was then measured in NK-cell subsets in the bone marrow. We chose this short-pulse protocol to minimize the transition of BrdU-positive NK cells from one stage of differentiation to the other. At steady state (day 0, Figure 4A), DN NK cells displayed the greater rate of proliferation, followed by $CD11b^{low}$

Table 1. Transcription factors up-regulated in CD11b^{low} NK cells on NK-cell maturation

Probe set	Unigene ID	Gene title	Gene symbol
1430435_at	Mm.336679	AF4/FMR2 family, member 3	<i>Aff3</i>
1416135_at	Mm.203	Apurinic/apyrimidinic endonuclease 1	<i>Apex1</i>
1419959_s_at	NA	RIKEN cDNA C330003B14 gene	<i>C330003B14Rik</i>
1441579_at	Mm.130167	Doublesex and mab-3 related transcription factor like family A1	<i>Dmrta1</i>
1441107_at	Mm.32825	Doublesex and mab-3 related transcription factor like family A2	<i>Dmrta2</i>
1440551_at	Mm.246674	DnaJ (Hsp40) homolog, subfamily C, member 1	<i>Dnajc1</i>
1437187_at	Mm.11747	E2F transcription factor 7	<i>E2f7</i>
1418635_at	Mm.219460	ets variant gene 3	<i>Etv3</i>
1417541_at	Mm.57223	Helicase, lymphoid specific	<i>Hells</i>
1426114_at	NA	Heterogeneous nuclear ribonucleoprotein A/B	<i>Hnrpab</i>
1439998_at	NA	Jumonji domain containing 1C	<i>Jmjd1c</i>
1417394_at	Mm.4325	Kruppel-like factor 4 (gut)	<i>Klf4</i>
1418936_at	Mm.86646	v-maf musculoaponeurotic fibrosarcoma oncogene family, protein F (avian)	<i>Maff</i>
1446570_at	Mm.116898	Mastermind-like 2 (<i>Drosophila</i>)	<i>Maml2</i>
1439065_x_at	Mm.270762	Similar to zinc finger protein 665	<i>MGC117846</i>
1421317_x_at	Mm.52109	Myeloblastosis oncogene	<i>Myb</i>
1424942_a_at	Mm.2444	Myelocytomatosis oncogene	<i>Myc</i>
1420710_at	Mm.4869	Reticuloendotheliosis oncogene	<i>Rel</i>
1436325_at	NA	RAR-related orphan receptor alpha	<i>Rora</i>
1427677_a_at	Mm.434350	SRY-box containing gene 6	<i>Sox6</i>
1429951_at	Mm.343095	Single-stranded DNA binding protein 2	<i>Ssbp2</i>
1433471_at	Mm.31630	Transcription factor 7, T-cell specific	<i>Tcf7</i>
1453076_at	Mm.6922	RIKEN cDNA 913021103 gene	<i>913021103Rik</i>

From the gene expression analysis described in Figure 3, differentially expressed transcription factors were identified.

NK cells, whereas DP and CD27^{low} NK cells displayed low proliferative capacities (Figure 4A). During NK-cell replenishment, the proliferation of all NK-cell subsets was increased (Figure 4B), but NK-cell subsets ranked in the same order as in steady-state conditions comparing their proliferation, although the statistics were less significant. As expected, most CD122⁺ NK-cell precursors (NKp) were also found to be BrdU positive (data not shown). Thus, the proliferative potential of NK-cell subsets decreased as follows: NKp > DN > CD11b^{low} > DP > CD27^{low}, further supporting that NK-cells differentiate according to this developmental path.

Adoptive transfers support a DN → CD11b^{low} → DP → CD27^{low} pathway of differentiation

The capacity of each NK-cell subset to give rise to the other cell subsets was also assessed using adoptive transfer settings. For this, we sorted NK-cell subsets from NDE mice according to CD11b, CD27, and EGFP expression (Figure 5A) and adoptively transferred them individually into unirradiated adult C57BL/6 mice. Two weeks later, transferred cells and their progeny were identified in the spleen of recipient mice on the basis of EGFP, and we measured their levels of

Table 2. Transcription factors up-regulated in CD27^{low} NK cells on NK-cell maturation

Probe set	Unigene ID	Gene title	Gene symbol
1455621_at	Mm.26636	cDNA sequence BC066107	<i>BC066107</i>
1438757_at	Mm.129275	RIKEN cDNA C130069I09 gene	<i>C130069I09Rik</i>
1455334_at	Mm.41364	RIKEN cDNA D330038O06 gene	<i>D330038O06Rik</i>
1422537_a_at	Mm.34871	Inhibitor of DNA binding 2	<i>Id2</i>
1416714_at	Mm.334861	Interferon regulatory factor 8	<i>Irf8</i>
1439846_at	NA	Kruppel-like factor 12	<i>Klf12</i>
1448890_at	Mm.26938	Kruppel-like factor 2 (lung)	<i>Klf2</i>
1452001_at	Mm.255151	Nuclear factor, erythroid derived 2	<i>Nfe2</i>
1416542_at	Mm.258953	PHD finger protein 1	<i>Phf1</i>
1447864_s_at	Mm.192094	pogo transposable element with KRAB domain	<i>Pogk</i>
1418622_at	Mm.397471	RAB2, member RAS oncogene family	<i>Rab2</i>
1449361_at	Mm.94519	T-box 21	<i>Tbx21</i>
1432158_a_at	Mm.279752	Trafficking protein particle complex 2	<i>Trappc2</i>
1443880_at	Mm.27258	Zinc finger and BTB domain containing 39	<i>Zbtb39</i>
1422748_at	Mm.259595	Zinc finger homeobox 1b	<i>Zfhx1b</i>
1453212_at	Mm.333743	Zinc finger protein 383	<i>Zfp383</i>
1449414_at	Mm.42140	Zinc finger protein 53	<i>Zfp53</i>
1419239_at	Mm.12916	Zinc finger protein 54	<i>Zfp54</i>
1424261_at	Mm.72124	Zinc finger protein 672	<i>Zfp672</i>
1456324_at	Mm.422831	Zinc finger protein 748	<i>Zfp748</i>
1455945_at	NA	RIKEN cDNA A530094I17 gene	<i>A530094I17Rik</i>
1457566_at	Mm.33443	RIKEN cDNA A830058L05 gene	<i>A830058L05Rik</i>

From the gene expression analysis described in Figure 3, differentially expressed transcription factors were identified.

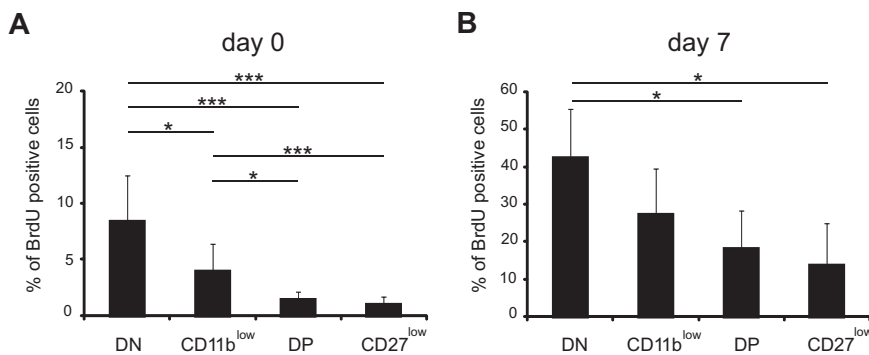


Figure 4. DN and CD11b^{low} NK cells display a high rate of proliferation. NDE mice were injected with phosphate-buffered saline (A) or DT (B) and injected with BrdU 7 days later. Six hours after BrdU injection, BrdU incorporation was measured in bone marrow NK-cell subsets by flow cytometry, as described in "Measurement of BrdU incorporation." Results show the mean \pm SD BrdU incorporation in each NK-cell subset; $n = 3$ experiments. Statistical comparisons between groups were performed using Mann-Whitney tests: * $P < .05$, *** $P < .001$.

CD27 and CD11b expression. As shown in Figure 5B, transferred DN NK cells gave rise to all NK-cell subsets; CD11b^{low} NK cells produced DP and CD27^{low} NK cells, DP NK cells yielded DP and CD27^{low} NK cells, and CD27^{low} NK cells remained CD27^{low}. These results show that DN NK cells are precursors of all other NK-cell subsets and strongly support the DN \rightarrow CD11b^{low} \rightarrow DP \rightarrow CD27^{low} model of NK-cell differentiation.

Discussion

Surface density of CD27 and CD11b subdivides mouse NK cells into 4 subsets: DN, CD11b^{low}, DP, and CD27^{low}.¹¹ Here, we first characterized the DN subset. DN NK cells belong to the NK-cell lineage as shown by their expression of activating receptors NKp46, NKG2D, and NK1.1, their high level of granzyme B, and their development in RAG^{-/-} mice. However, DN NK cells displayed a very immature phenotype, according to a scheme of maturation proposed earlier.²⁵ Indeed, DN cells expressed low levels of Ly49 receptors and DX5 but reciprocally high levels of IL-7R. They composed a fraction of the DX5^{low} population of NK cells previously found to express tumor necrosis factor-related apoptosis-inducing ligand and to be abundant in fetal and neonatal mice.⁹

The differentiation of CD11b^{low} NK cells into CD11b^{high} NK cells has been previously addressed by several groups using cell transfer into irradiated lymphopenic recipients.^{9,10,14,15} Irradiation of recipient mice clearly improves grafting of transferred cells. However, it can also induce "homeostatic" proliferation and phenotypic changes of transferred NK or T cells,^{16,26-28} which complicate the interpretation of such experiments. Here, we present compelling evidence that not only demonstrate the validity of the CD11b^{low} \rightarrow DP \rightarrow CD27^{low} model of NK-cell differentiation but also complete it with the description of DN NK cells. First, we used NDE mice, an experimental model that presents 2 important advantages: (1) it allows the monitoring of NK-cell development in the absence of cell transplantation; and (2) the tracking of NK cells can be performed by EGFP expression, avoiding the use of antibodies that may bind nonspecifically to other cells, an important issue when looking at very rare subsets. Using this unique protocol, we found that DN, CD11b^{low}, DP, and CD27^{low} subsets arise in a sequential manner on replenishment of the NK-cell pool in NDE animals. A similar chronology was observed when looking at developing NK cells after the first weeks of postnatal life in wild-type mice. These results suggest that DP and CD27^{low} NK cells differentiate from DN and/or from CD11b^{low} cells. In these experiments, no clear difference in the timing of appearance of DN and CD11b^{low} NK cells was observed, suggesting that these 2 cell types are closely related. Second, a global analysis of gene

expression profiles of CD11b^{low}, DP, and CD27^{low} revealed that CD11b^{low} and CD27^{low} NK cells are the most distant subsets and that DP cells display an intermediate gene profile between those 2 subsets. These transcriptomic analyses also revealed that CD11b^{low} and CD27^{low} NK cells differed mainly by their proliferative potential and by their effector functions. This dissociation is a general feature of cellular differentiation and can also be taken as a supportive evidence of the precursor nature of CD11b^{low} NK cells. These data were confirmed by measurements of BrdU incorporation by NK-cell subsets. Indeed, either at steady-state or during replenishment of the NK-cell pool, DN and CD11b^{low} NK cells displayed a higher proliferation rate than the other subsets, which confirms and extends previous findings.^{10,29} Importantly, DN NK cells proliferated more than CD11b^{low} NK cells but less than CD122⁺ NKp, suggesting that they represent an intermediate stage between NKp and CD11b^{low} NK cells. Finally, we sorted NK-cell subsets on the basis of EGFP, CD27, and CD11b expression and transferred them into normal nonirradiated recipients. Two weeks later, the analysis of transferred cells in the spleen of recipient mice demonstrated that DN NK cells could give rise to all other subsets, whereas this potential was gradually lost in other subsets: CD11b^{low} gave rise to themselves, DP and CD27^{low} NK cells, whereas DP gave rise to CD27^{low} and CD27^{low} remained CD27^{low}. Collectively, our data strongly suggest that mouse NK-cell maturation can be modeled in a 4-stage program with the following intermediates: DN \rightarrow CD11b^{low} \rightarrow DP \rightarrow CD27^{low}. CD27^{low} NK cells are probably the end stage of NK-cell differentiation before cell death, as suggested by a previous study that showed that KLRG1⁺ NK cells, which are mostly CD27^{low}, are very susceptible to spontaneous apoptosis on ex vivo isolation.³⁰ Importantly, CD27 has been recently shown to distinguish between 2 NK-cell subsets in human PBMCs. CD27^{high} and CD27^{low} NK cells corresponded to the previously described CD56^{bright} and CD56^{dim} NK cells,^{31,32} suggesting that CD27 is regulated similarly during mouse and human NK-cell differentiation. Early stages of NK-cell development have also been identified in human lymph nodes and tonsils that express low levels of the CD11b integrin, unlike mature NK cells.³³ Thus, the cell-surface density of CD11b and CD27 appears to be relevant in both mouse and human to dissect NK-cell developmental stages.

Where do NK cells mature and what are the signals involved? As presented here, and in previous reports, NK-cell subsets display some tissue preferences. It is therefore possible that tissue-specific environments impact on their differentiation. Dendritic cells could act as regulators of NK-cell maturation as they have already been shown to control NK-cell proliferation and effector functions.^{34,35}

Is there a functional specialization of the NK-cell subsets? For other leukocyte subsets, maturation stages have been associated with various functions. This has been shown for dendritic cells that have distinct but

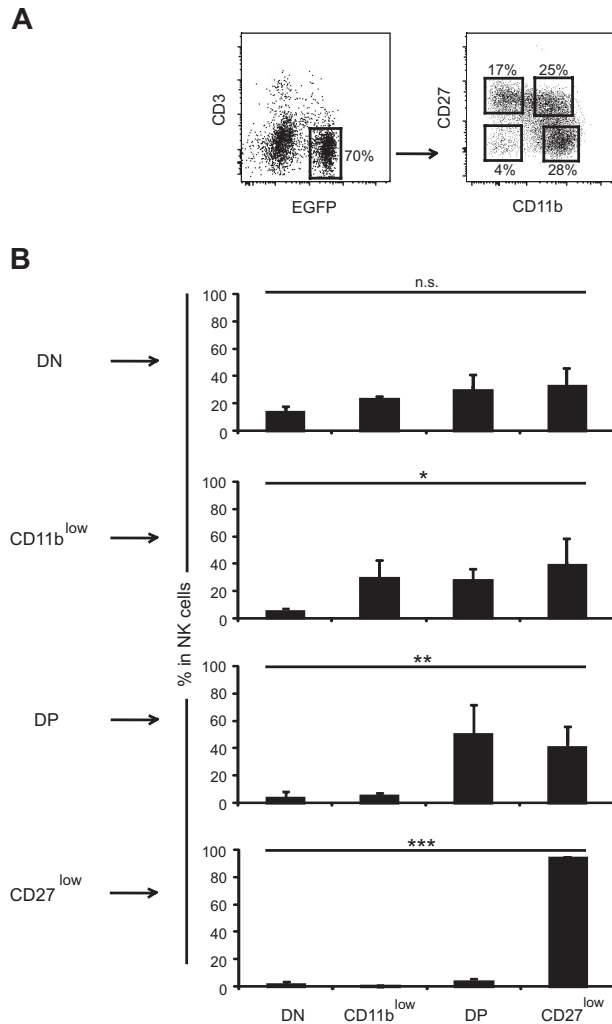


Figure 5. Adoptive transfers of sorted NK-cell subsets. (A) The 4 NK-cell subsets were sorted by flow cytometry from the spleen of NDE mice using the sorting gates. Cells were then individually transferred into unirradiated recipient mice. Fourteen days later, the progeny of transferred cells was tracked in the spleen of recipient mice thanks to EGFP expression. (B) Their expression of CD27 and CD11b was measured, and the frequency of each subset was calculated for each adoptive transfer, as indicated. Mean \pm SD of 3 independent experiments. We used a one-way analysis of variance test with posttest of linear trend to test whether there was a trend such that values increase as one moves from left to right (ie, from DN to CD27^{low}). This test gave significant results for all comparisons except for the transfer of DN NK cells, as predicted if DN NK cells were precursors of the other subsets. n.s. indicates not significant. * $P < .05$, ** $P < .01$, *** $P < .001$.

complementary functions in antigen presentation.³⁶ In an attempt to address this issue, we compared gene expression profiles between CD11b^{low} and CD27^{low} NK cells. CD11b^{low} NK cells were found to

preferentially express genes involved in “organogenesis,” such as lymphotoxins or bone morphogenetic proteins. Moreover, we found that DN NK cells expressed ROR γ t transcripts at high levels (data not shown). This suggests that immature NK cells may share organogenetic properties with lymphoid tissue inducer cells, an issue that starts to be appreciated.^{23,37-40} The most striking difference between CD11b^{low} and CD27^{low} NK cells according to gene profiling analysis was the dissociation between proliferative capacity and effector functions. Indeed, “cell cycle” was the most significant term found associated with the signature of the CD11b^{low} subset, whereas, conversely, genes involved in effector functions, such as cytotoxicity, were up-regulated in CD27^{low} NK cells. This result suggests that the specific function of DN/CD11b^{low} NK cells is probably to act as precursors capable of giving rise to effector cells when needed. Their low number in all organs supports this conclusion. However, DP and CD27^{low} NK cells are also clearly capable of proliferating as shown by BrdU experiments, suggesting that these more differentiated NK cells can also contribute to NK-cell expansion in case of inflammation. Regarding their effector functions, DP and CD27^{low} NK cells, which are very abundant in all organs, have been shown to exhibit comparable ex vivo responses to cytokines or cross-linking of activating receptors¹³ but to express different chemotactic receptors.¹¹⁻¹³ Further studies will be required to determine whether these 2 subsets have specific roles during immune responses.

Acknowledgments

E.V.'s laboratory is supported by the European Union (FP6, LSHB-CT-2004-503319-Allotem), Ligue Nationale contre le Cancer (Equipe labellisée La Ligue), Agence Nationale de la Recherche, Institut National du Cancer, Institut National de la Santé et de la Recherche Médicale, Centre National de la Recherche Scientifique, and Ministère de l'Enseignement Supérieur et de la Recherche. E.V. is a scholar of the Institut Universitaire de France. L.C. is sponsored by Institut National du Cancer.

Authorship

Contribution: L.C., T.W., and E.V. designed the research; L.C., N.F., J.C., C.R., and T.W. performed experiments; and L.C., T.W., and E.V. wrote the manuscript.

Conflict-of-interest disclosure: N.F. is an employee of Innate-Pharma. E.V. is a founder and shareholder of Innate-Pharma. The remaining authors declare no competing financial interests.

Correspondence: Thierry Walzer or Eric Vivier, CIML CNRS-Inserm-Université de la Méditerranée, Campus de Luminy, Case 906, 13288 Marseille Cedex 09, France; e-mail: walzer@ciml.univ-mrs.fr or vivier@ciml.univ-mrs.fr.

References

- Moretta L, Bottino C, Pende D, Mingari MC, Biassoni R, Moretta A. Human natural killer cells: their origin, receptors and function. *Eur J Immunol*. 2002;32:1205-1211.
- Vivier E, Tomasello E, Baratin M, Walzer T, Ugolini S. Functions of natural killer cells. *Nat Immunol*. 2008;9:503-510.
- Lanier LL. NK cell recognition. *Annu Rev Immunol*. 2005;23:225-274.
- Moretta L, Moretta A. Unravelling natural killer cell function: triggering and inhibitory human NK receptors. *EMBO J*. 2004;23:255-259.
- Raulet DH. Missing self recognition and self tolerance of natural killer (NK) cells. *Semin Immunol*. 2006;18:145-150.
- Caligiuri MA. Human natural killer cells. *Blood*. 2008;112:461-469.
- Ferlazzo G, Thomas D, Lin SL, et al. The abundant NK cells in human secondary lymphoid tissues require activation to express killer cell Ig-like receptors and become cytolytic. *J Immunol*. 2004;172:1455-1462.
- Lanier LL, Le AM, Civin CI, Loken MR, Phillips JH. The relationship of CD16 (Leu-11) and Leu-19 (NKH-1) antigen expression on human peripheral blood NK cells and cytotoxic T lymphocytes. *J Immunol*. 1986;136:4480-4486.
- Takeda K, Cretney E, Hayakawa Y, et al. TRAIL identifies immature natural killer cells in newborn mice and adult mouse liver. *Blood*. 2005;105:2082-2089.
- Kim S, Iizuka K, Kang HS, et al. In vivo developmental stages in murine natural killer cell maturation. *Nat Immunol*. 2002;3:523-528.
- Hayakawa Y, Smyth MJ. CD27 dissects mature NK cells into two subsets with distinct responsiveness and migratory capacity. *J Immunol*. 2006;176:1517-1524.
- Gregoire C, Chasson L, Luci C, et al. The trafficking of natural killer cells. *Immunol Rev*. 2007;220:169-182.
- Walzer T, Chiossone L, Chaix J, et al. Natural

- killer cell trafficking in vivo requires a dedicated sphingosine 1-phosphate receptor. *Nat Immunol*. 2007;8:1337-1344.
14. Hayakawa Y, Huntington ND, Nutt SL, Smyth MJ. Functional subsets of mouse natural killer cells. *Immunol Rev*. 2006;214:47-55.
 15. Roth C, Carlyle JR, Takizawa H, Raulet DH. Clonal acquisition of inhibitory Ly49 receptors on developing NK cells is successively restricted and regulated by stromal class I MHC. *Immunity*. 2000;13:143-153.
 16. Murali-Krishna K, Ahmed R. Cutting edge: naive T cells masquerading as memory cells. *J Immunol*. 2000;165:1733-1737.
 17. Walzer T, Blery M, Chaix J, et al. Identification, activation, and selective in vivo ablation of mouse NK cells via NKp46. *Proc Natl Acad Sci U S A*. 2007;104:3384-3389.
 18. Dennis G Jr, Sherman BT, Hosack DA, et al. DAVID: Database for Annotation, Visualization, and Integrated Discovery. *Genome Biol*. 2003;4:P3.
 19. National Center for Biotechnology Information. GEO: Gene Expression Omnibus. <http://www.ncbi.nlm.nih.gov/geo>. Accessed February 10, 2009.
 20. Stewart CA, Walzer T, Robbins SH, Malissen B, Vivier E, Prinz I. Germ-line and rearranged Tcrd transcription distinguish bona fide NK cells and NK-like gammadelta T cells. *Eur J Immunol*. 2007;37:1442-1452.
 21. Xiao C, Calado DP, Galler G, et al. MiR-150 controls B cell differentiation by targeting the transcription factor c-Myb. *Cell*. 2007;131:146-159.
 22. Takahashi K, Yamanaka S. Induction of pluripotent stem cells from mouse embryonic and adult fibroblast cultures by defined factors. *Cell*. 2006;126:663-676.
 23. Luci C, Reynders A, Ivanov II, et al. Influence of the transcription factor RORgammat on the development of NKp46+ cell populations in gut and skin. *Nat Immunol*. 2009;10:75-82.
 24. Sullivan BM, Juedes A, Szabo SJ, Von Herrath M, Glimcher LH. Antigen-driven effector CD8 T cell function regulated by T-bet. *Proc Natl Acad Sci U S A*. 2003;100:15818-15823.
 25. Colucci F, Caligiuri MA, Di Santo JP. What does it take to make a natural killer? *Nat Rev Immunol*. 2003;3:413-425.
 26. Ranson T, Vosshenrich CA, Corcuff E, Richard O, Muller W, Di Santo JP. IL-15 is an essential mediator of peripheral NK-cell homeostasis. *Blood*. 2003;101:4887-4893.
 27. Jamieson AM, Isnard P, Dorfman JR, Coles MC, Raulet DH. Turnover and proliferation of NK cells in steady state and lymphopenic conditions. *J Immunol*. 2004;172:864-870.
 28. Prlic M, Blazar BR, Farrar MA, Jameson SC. In vivo survival and homeostatic proliferation of natural killer cells. *J Exp Med*. 2003;197:967-976.
 29. Huntington ND, Tabarias H, Fairfax K, et al. NK cell maturation and peripheral homeostasis is associated with KLRG1 up-regulation. *J Immunol*. 2007;178:4764-4770.
 30. Robbins SH, Tessmer MS, Mikayama T, Brossay L. Expansion and contraction of the NK cell compartment in response to murine cytomegalovirus infection. *J Immunol*. 2004;173:259-266.
 31. Silva A, Andrews DM, Brooks AG, Smyth MJ, Hayakawa Y. Application of CD27 as a marker for distinguishing human NK cell subsets. *Int Immunol*. 2008;20:625-630.
 32. Vossen MT, Matmati M, Hertoghs KM, et al. CD27 defines phenotypically and functionally different human NK cell subsets. *J Immunol*. 2008;180:3739-3745.
 33. Freud AG, Yokohama A, Becknell B, et al. Evidence for discrete stages of human natural killer cell differentiation in vivo. *J Exp Med*. 2006;203:1033-1043.
 34. Hochweller K, Striegler J, Hammerling GJ, Garbi N. A novel CD11c.DTR transgenic mouse for depletion of dendritic cells reveals their requirement for homeostatic proliferation of natural killer cells. *Eur J Immunol*. 2008;38:2776-2783.
 35. Lucas M, Schachterle W, Oberle K, Aichele P, Diefenbach A. Dendritic cells prime natural killer cells by trans-presenting interleukin 15. *Immunity*. 2007;26:503-517.
 36. Thery C, Amigorena S. The cell biology of antigen presentation in dendritic cells. *Curr Opin Immunol*. 2001;13:45-51.
 37. Cella M, Fuchs A, Vermi W, et al. A human natural killer cell subset provides an innate source of IL-22 for mucosal immunity. *Nature*. 2009;457:722-725.
 38. Cupedo T, Crellin NK, Papazian N, et al. Human fetal lymphoid tissue-inducer cells are interleukin 17-producing precursors to RORc+ CD127+ natural killer-like cells. *Nat Immunol*. 2009;10:66-74.
 39. Sanos SL, Bui VL, Mortha A, et al. RORgammat and commensal microflora are required for the differentiation of mucosal interleukin 22-producing NKp46+ cells. *Nat Immunol*. 2009;10:83-91.
 40. Satoh-Takayama N, Vosshenrich CA, Lesjean-Pottier S, et al. Microbial flora drives interleukin 22 production in intestinal NKp46+ cells that provide innate mucosal immune defense. *Immunity*. 2008;29:958-970.